PROCEEDINGS OF SCIENCE

Deep images at metre wavelengths using the GMRT

S. K. Sirothia*
NCRA-TIFR, India
E-mail: sirothia@ncra.tifr.res.in

D. J. Saikia
NCRA-TIFR, India
E-mail: djs@ncra.tifr.res.in

D. Burgarella
Observatoire Astronomique Marseille Provence, Laboratoire d'Astrophysique de Marseille, France
E-mail: denis.burgarella@oamp.fr

We have been studying several fields at low radio frequencies, such as ELAIS-N1, GOODS-N/S and the AKARI deep field, and making deep images at metre-wavelengths using the Giant Metre-wave Radio Telescope (GMRT). In this paper we largely summarise the results of the observations of ELAIS-N1 at 325 MHz, and present new results on the ECDFS at 150 and 325 MHz. These fields have been studied extensively at different wave-bands using the most powerful ground-based and space telescopes. The ELAIS-N1 image with the GMRT has an rms noise of $\sim$40 μJy beam^{-1} towards the phase centre, while for the ECDFS field the rms noise values are 2.5 mJy beam^{-1} and 75μJy beam^{-1} at 150 and 325 MHz respectively. The ECDFS observations also show a flattening of the source counts at $\sim$1 mJy at 325 MHz, consistent with the results reported earlier for the ELAIS-N1 field. The sub-mJy sources show a larger scatter in their spectral indices which is possibly at least partly due to a population of both starburst galaxies and low-luminosity AGN. These deep observations with the GMRT have helped identify a significant number of very steep-spectrum sources, which could be either relic sources or candidate high-redshift galaxies.

ISKAF2010 Science Meeting - ISKAF2010
June 10-14, 2010
Assen, the Netherlands

*Speaker.

PoS(ISKAF2010)051

1. Introduction

A fundamental issue in extragalactic studies is to understand the evolution of galaxies, namely their star formation history, formation of active galactic nuclei (AGNs), building-up of large disks and bulges and the formation and evolution of supermassive black holes (SMBHs). A number of different physical processes are expected to play significant roles. For example, merging of galaxies could trigger collapse of molecular clouds and star formation, often in dusty environments, while AGN occur due to the accretion of gas onto SMBHs. These processes exhibit signatures across the electromagnetic spectrum, making it essential to make multiwavelength studies to understand the properties, formation and evolution of galaxies over cosmic time [1, 2].

At radio wavelengths, the extragalactic radio source population ranges from normal galaxies with luminosities $\sim 10^{17}$ W Hz^{-1} at $\sim$1400 MHz to the luminous radio galaxies and quasars whose radio luminosity could be larger by a factor of $\sim 10^{8}$. The radio galaxies and quasars are powered by an AGN and usually consist of two lobes of synchrotron radio emission on either side of the central nucleus, and could range in size from less than $\sim$10 pc to over a few Mpc. In addition, radio emission is also detected from regions of massive star formation, which consist of both thermal free-free and synchrotron emission, the latter being dominant at low radio frequencies (less than $\sim$1 GHz). The radio sources with a flux density greater than $\sim$1 mJy at 1400 MHz are almost entirely due to an AGN which is powered by accretion onto a SMBH. However, below $\sim$1 mJy the radio emission is increasingly due to synchrotron emission from relativistic electrons generated in supernovae in regions of massive star formation, and perhaps also a population of low-luminosity AGN [3, 4, 5, 6]. The star formation in these galaxies could be triggered by interactions and mergers, and thereby contain an imprint of the evolution of the galaxy over cosmic time. Massive star formation produces radiation across a large wavelength range, and it is known that the radio emission in star-forming galaxies is strongly correlated with the infrared emission perhaps upto redshifts of $\sim$2 [7, 8], and possibly with the X-ray emission in nearby galaxies [9].

Radio emission sees through the gas and dust which lie in the central regions of active galaxies, and has played an important role in distinguishing between AGN- and starburst-dominated galaxies, although both these forms of activity could co-exist in a given galaxy. At low radio frequencies, the emission is almost entirely non-thermal, and in principle could be a useful tracer of radiation from old electrons. Besides providing useful diagnostics for distinguishing between AGN- and starburst-dominated galaxies, low-frequency radio observations help determine their spectral indices over a large frequency range and help identify very steep-spectrum sources, with spectral indices $\alpha > 1.3$ ($S \propto \nu^{-\alpha}$), which could be either high-redshift galaxies [10] or relic sources [11]. These observations are critical for studying episodic activity in AGN [12, 18], and provide valuable information towards understanding the evolution of galaxies over cosmic time.

2. GMRT observations of selected fields

To explore some of the issues related to galaxy formation and evolution and possible relationships between AGN and starburst activity, we have been making deep observations of several selected fields at low radio frequencies using the Giant Metrewave Radio Telescope (GMRT). The fields were chosen so that these were well studied at different wavebands, and includes the northern

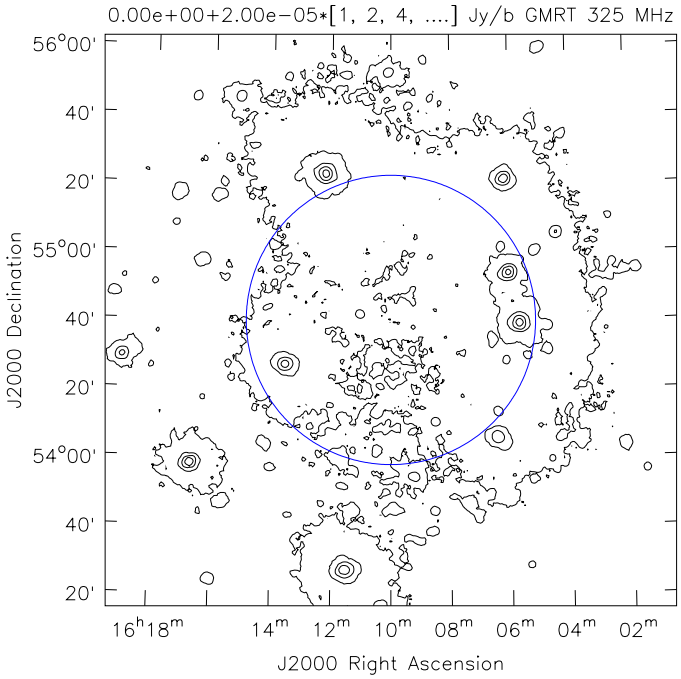

Figure 1: The variation of rms noise across the image before the primary beam correction for the ELAIS-N1 field reproduced from Sirothia et al. [13]. In this figure and in all the images presented here the contour levels in units of Jy beam^{-1} are represented by mean+rms$\times$(n) where n is the multiplication factor. These levels are shown above each image. All negative contours appear as dashed lines.

field of the European Large Area Infrared Space Observatory (ISO) Survey (ELAIS-N1), the Great Observatories Origins Deep Survey (GOODS-N/S) and AKARI fields.

2.1 ELAIS-N1

The ELAIS-N1 field has been chosen in a region of the sky with low-IR foreground emission, to allow detection of fainter and possibly more distant galaxies. GMRT observations of the ELAIS-N1 field at 325 MHz were made on two different days by pointing towards the centre of the field ($16^{\rm h}10^{\rm m}$, $+54^\circ36'$). The final image made by combining the data of both the days has a median rms noise figure of $\sim$40 μJy beam^{-1} towards the centre of the field, and is amongst the deepest images made at this frequency [13]. In order to help in the identification of radio frequency interference (RFI) and minimize smearing effects, the data were acquired with a small visibility integration time from the correlator. The variation of rms noise across the image before primary beam correction is shown in Figure 1, while the GMRT image of an area of 30$\times$30 arcmin^2 from our observations at 325 MHz, and for comparison, the corresponding images of the same area at 610 MHz with the GMRT from Garn et al. [14] and the Faint Images of the Radio Sky at Twenty-centimetres (FIRST) and NRAO VLA Sky Survey (NVSS) at 1400 MHz are shown in Figure 2. Although the brighter sources are seen clearly in all the images, many more sources are seen in the 325-MHz image due to the deeper surface brightness sensitivity of this image. To further illustrate the sources found in this deep image, we show our image at 325 MHz of a highly asymmetric double-lobed source

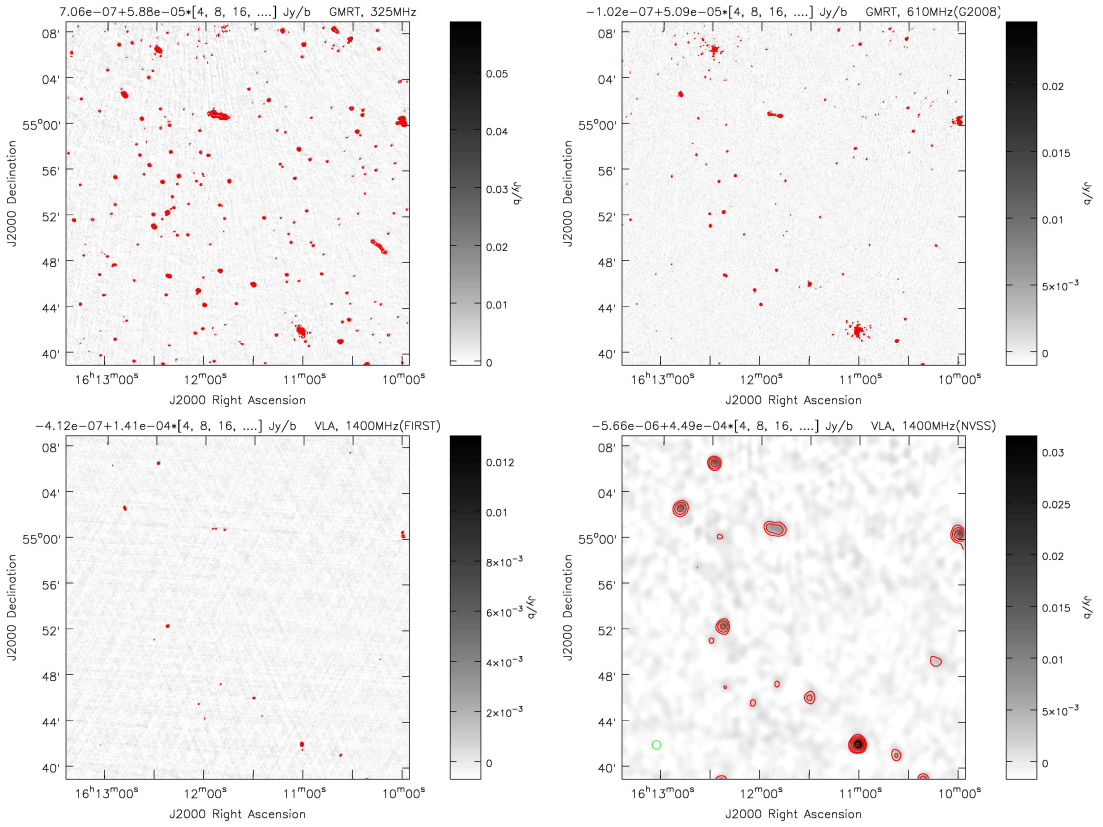

Figure 2: GMRT image of an area of 30×30 arcmin^2 from our observations at 325 MHz (top left), and the corresponding images of the same area at 610 MHz with the GMRT [14] (top right), and from FIRST (bottom left) and NVSS (bottom right) at 1400 MHz, reproduced from [13].

with a possible core in Figure 3, and the corresponding images of the same source at 610 MHz with the GMRT from Garn et al., and from FIRST and NVSS at 1400 MHz. The highly sensitive 325-MHz image has clearly shown both lobes of this highly-asymmetric double, revealing details of the structural information, not apparent in the other images.

2.2 ECDFS

The Extended Chandra Deep Field−South (ECDFS) is one of the most extensively studied regions of the sky, and has been observed at a number of wavebands using some of the most powerful ground-based and space telescopes. With the large amount of multiwavelength data which is available, this field is valuable for studying issues of galaxy evolution, and tracing their star formation and AGN history. The GMRT observations at 153 and 325 MHz which we present here are from archival data initially proposed by Udaya Shankar et al. (14NUS01) and Jose Afonso et al. (09JAa01) respectively. These observations were made with bandwidths of 5.6 and 32 MHz respectively, and with pointing centres at $03^{\rm h}\ 32^{\rm m}\ -28^\circ16'$ and $03^{\rm h}33^{\rm m}00^{\rm s}.5\ -27^\circ41'04''$ respectively. The duration of the observations at 153 MHz was ∼4 hr compared with ∼40 hr at 325 MHz. The median rms noise in the central region is 2.5 mJy beam^{-1} at 153 MHz and 75μJy beam^{-1} at

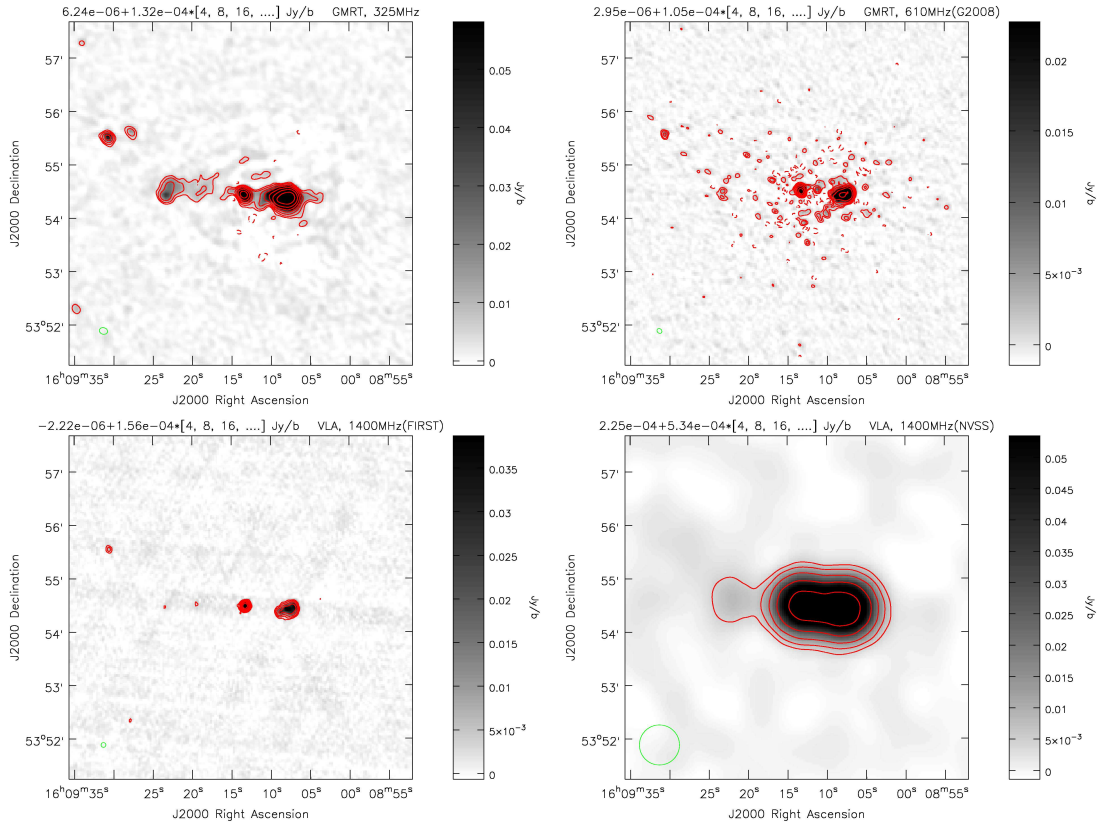

Figure 3: GMRT image at 325 MHz of a highly asymmetric double-lobed source with a possible core (top left), and the corresponding images of the same region at 610 MHz with the GMRT [14] (top right), and from FIRST (bottom left) and NVSS (bottom right) at 1400 MHz, reproduced from [13].

325 MHz. The images with angular resolutions of 25.2×14.5 arcsec^2 along a position angle (PA) of 24°, and 10.8×7.3 arcsec^2 along a PA 0f 16° are shown in Figure 4, along with a VLA image at 1400 MHz from Miller et al. [15]. The total numbers of sources detected within the half-power beam-width (HPBW) of 1.5° radius at 153 MHz and 0.7° radius at 325 MHz are 438 and 667 respectively.

To illustrate the range of structures, the GMRT images of four of the galaxies from the ECDFS field, are shown in Figure 5 along with their VLA images at 1400 MHz. These sources have spectroscopic redshifts available. While J033228-274355 appears to be an asymmetric double-lobed source with a jet-like structure towards the north, J033237-275004 is a single compact source at a redshift of 3.7638. J033242-273817 is at a redshift of 2.7301 and is the most luminous source known in our sample, while J033219-275408 is at a redshift of 0.9640. Although three of the four images shown here have a double-lobed structure, most of the sources in our sample are single sources.

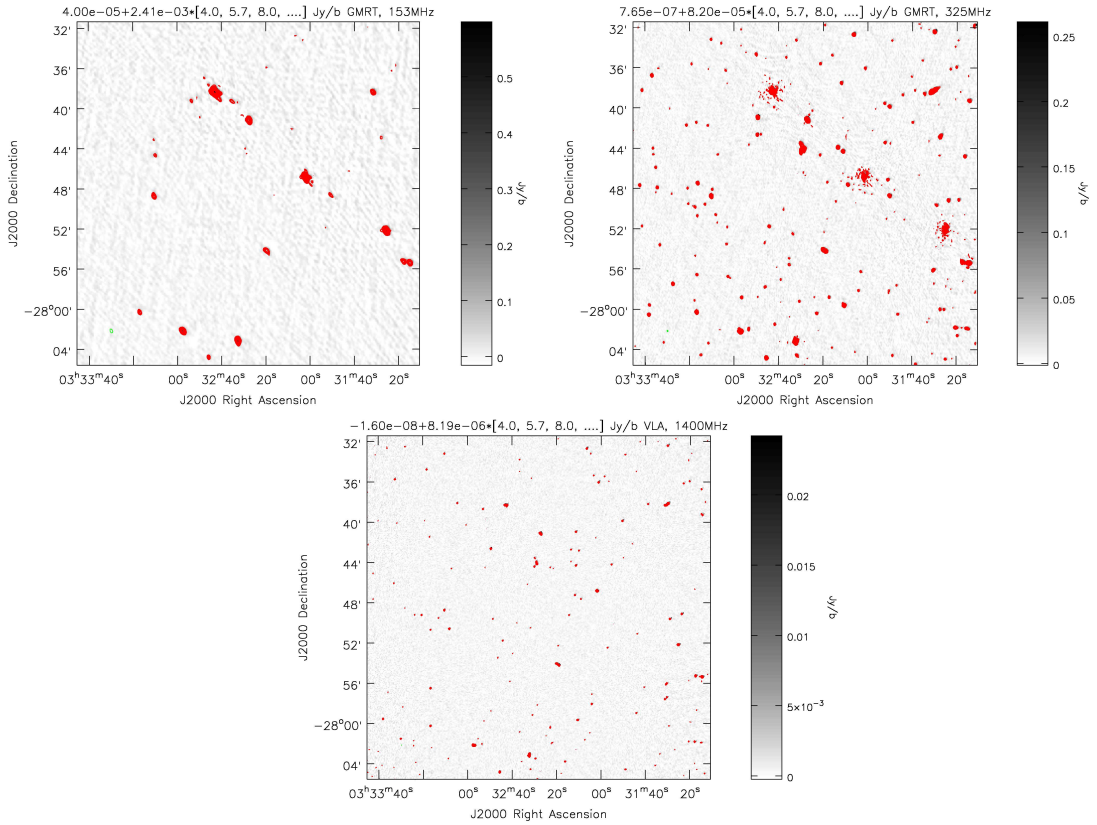

Figure 4: GMRT images at 153 MHz (top-left) and 325-MHz (top right) of the ECDFS field, along with the VLA 1400-MHz image (bottom) made from the data release of Miller et al. [15].

3. Spectral indices

We have estimated the spectral indices of the sources detected in the low-frequency observations of both the ELAIS-N1 and ECDFS fields. For ELAIS-N1, the spectral indices for the sources which are within 0.7° of the phase centre, the HPBW at 325 MHz, and which also appear either in the catalogues of Garn et al. or FIRST have been estimated. Although the resolutions of the observations at the different frequencies should ideally be the same, we have chosen those which are within a factor or two. The total number of sources in our sample is 844, while the corresponding numbers in the Garn et al. and FIRST catalogues within this distance are 553 and 134 respectively. The methodology used for matching the sources have been described in more detail by Sirothia et al. [13]. Only 360 of the 553 sources at 610 MHz have a match at 325 MHz, while 126 of the 134 sources at 1400 MHz have a match at 325 MHz. Sometimes sources which are listed as two independent sources at the higher frequency appear as a single source due to the detection of a bridge emission at the lower frequency. Both sensitivity and spectral indices of sources could be responsible for sources not having a match in the catalogues. The median value of α_{325}^{1400} for sources in the ELAIS-N1 field is 0.83, with four candidate Giga-Hertz Peaked Spectrum (GPS) sources and 30 very steep spectrum objects with $\alpha > 1.3$. In the ECDFS field we identify a further 19 sources with a very steep spectrum.

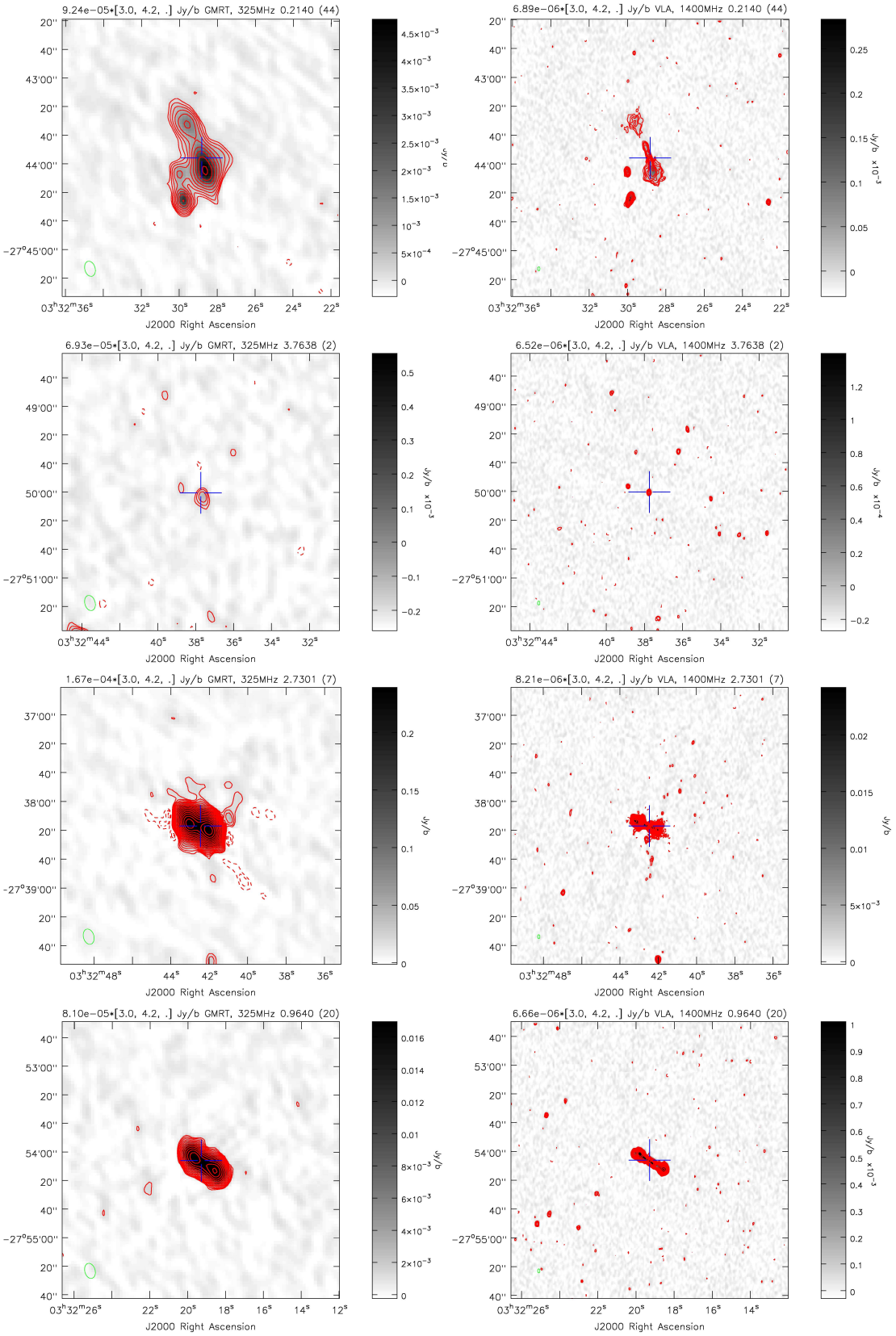

Figure 5: Our GMRT 325-MHz images are shown along with the VLA 1400-MHz images which have been plotted from the image of Miller et al. [15] for four of the sources in the ECDFS field. The redshift for each of the source is also indicated at the top right corner of the images.

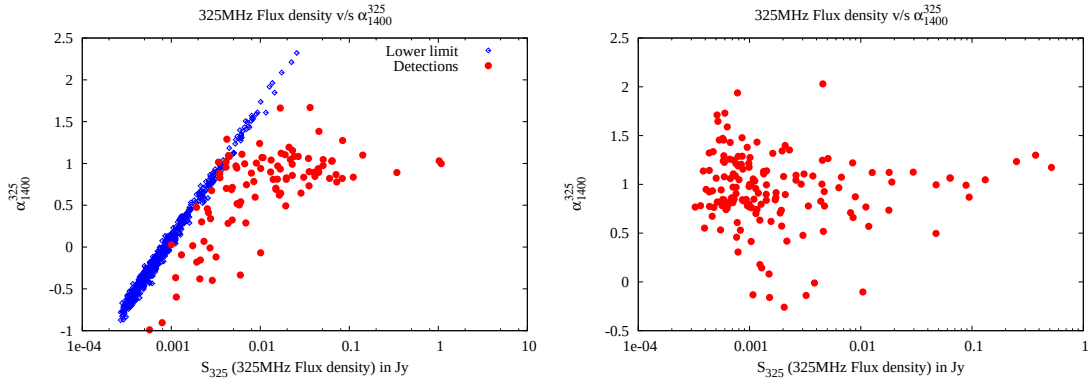

Figure 6: The spectral index vs flux density for the ELAIS-N1 (left) and ECDFS (right) sources.

3.1 Spectral index vs flux density

Possible dependence of spectral index on flux density may contain information on different populations of sources at different flux density levels, besides constraining models on evolution of source properties with cosmic epoch. For example, at flux densities significantly greater than $\sim$1 mJy, the source population is dominated by double-lobed radio galaxies and quasars where the optically thin emission appears correlated with luminosity and/or redshift, while the weaker source population consists of both starburst galaxies with low-frequency spectral indices in the range of $\sim$0.5$-$0.8, and low-luminosity AGN with spectral indices $<$0.5, when the emission is dominated by the nuclear or core radio emission. The plot of α^{1400}_{325} vs flux density at 325 MHz for the ELAIS-N1 field is shown in Figure 6. Since a large fraction of sources in this field have limits to their spectral indices, it is difficult to determine any dependence of spectral index on flux density. Deeper observations are required at the higher frequency, which is available for the ECDFS field. A similar plot for the ECDFS field shown in Figure 6, shows that most of the sources have $\alpha > 0.5$, with a median value of 0.95, and that there is a larger scatter in the values of spectral indices for sources below a mJy. This is possibly due to a combination of both different populations of sources at low flux densities and larger errors in the spectral indices at low flux densities. The number of flat-spectrum sources are almost always less than $\sim$5 mJy, which is not surprising since these are expected to be weak at low frequencies due to absorption effects. The figure does not show a significant dependence of spectral index on flux density for these sources.

In Figure 7 we present the spectral index vs redshift and radio luminosity for the sources from the ECDFS observations which have spectroscopic redshifts. Sources were considered to be identified with an optical object if the latter was within 10 arcsec of a radio component at 325 MHz, and within 2 arcsec of a radio component at 1400 MHz. Although this could miss large radio sources without a core component, it should not significantly affect the figure since most radio sources are small and single. Unlike in the case of radio-selected complete samples of radio galaxies and quasars, there is no significant correlation with either redshift or luminosity. Nearly half the sources in the figure have a flux density at 325 MHz which is below a mJy, where both starburst galaxies and low-luminosity AGN are expected to contribute to the source population.

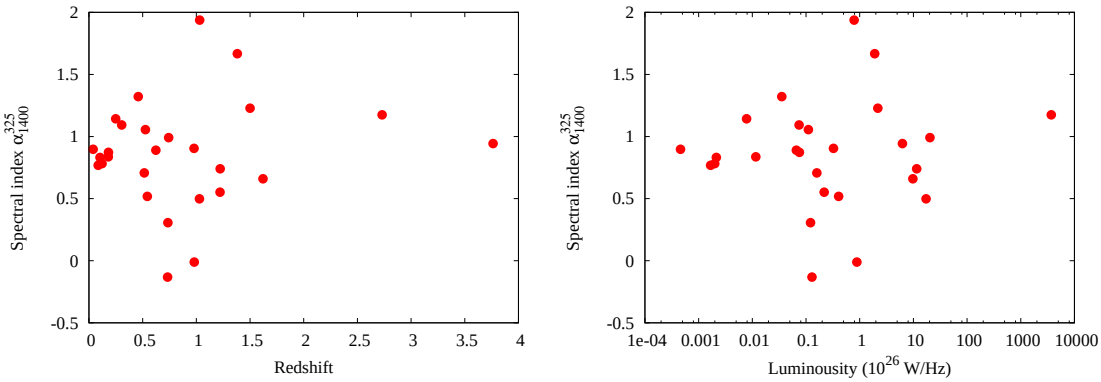

Figure 7: The spectral index vs redshift (left) and radio luminosity (right) for a sample of ECDFS sources with spectroscopic redshifts.

4. Source counts

The source counts at 325 MHz for the ELAIS-N1 field has been reported earlier by Sirothia et al. [13], where they had binned the sources in different ranges of flux density starting from 315 μJy. The typical peak flux density of the sources in even the lowest flux density bin was about 8 times the local rms value. The source counts were corrected for the fraction of the area over which the source could be detected because of the increased noise near bright sources. The normalized differential source counts showed a flattening at about a mJy, which had been seen earlier in only higher-frequency studies. In Figure 8, we show the normalized differential source counts for the ECDFS observations, along with those obtained earlier from the ELAIS-N1 observations [13]. The source counts from the two fields are consistent. A comparison with the functional form fitted by Wieringa [16] to the differential source counts ranging from about 4 mJy to 1 Jy from his deep 325-MHz Westerbork survey, shows clearly the flattening of the source counts at $\sim$1 mJy at 325 MHz. A more detailed modeling of the source counts is in progress. We reproduce here the source counts at 150 MHz for the LBDS-Lynx region from GMRT observations as well as from 7C observations from Ishwara-Chandra et al. [17] in Figure 9. The GMRT and 7C values are consistent at flux densities over $\sim$100 mJy. Deeper observations, possibly with LOFAR, are required for determining the flattening of the source counts at 150 MHz.

5. Concluding remarks

Deep images at low radio frequencies have helped determine their spectra over a large frequency range providing additional information to distinguish between AGN and starburst activity, These observations have shown a flattening of the source counts at low flux densities which is possibly due to a population of both starburst galaxies and low-luminosity AGN, and have helped identify many very steep-spectrum and several weak GPS sources. The very steep-spectrum sources could be high-redshift galaxies or relic radio sources and are being investigated further. It would be interesting to identify a larger sample of weak GPS sources and enquire whether their evolutionary paths are similar to those of the more luminous ones identified from strong radio source surveys.

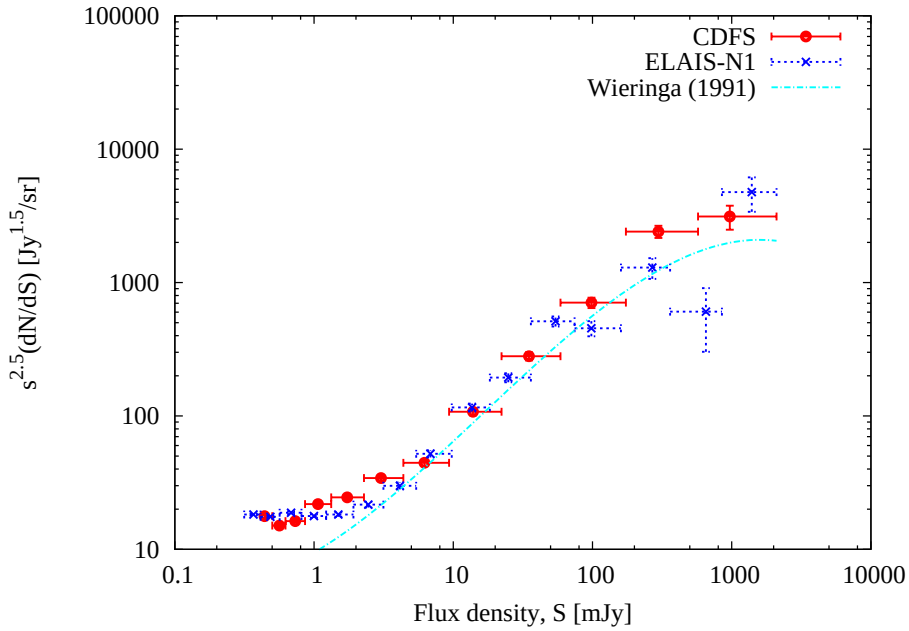

Figure 8: The normalized differential source counts at 325 MHz for the ELAIS-N1 [13] and ECDFS fields.

Acknowledgments

We thank our colleagues and collaborators, especially Michel Dennefeld, Herve Dole, Gopal-Krishna, Francois Ricquebourg, Jacques Roland and Udaya Shankar, for their inputs and comments during various stages of this work.

References

[1] P. Madau, L. Pozzetti and M. Dickinson, *The Star Formation History of Field Galaxies*, *ApJ*, **498**, 106, 1998

[2] A.M. Hopkins, J.F. Beacom, *On the Normalization of the Cosmic Star Formation History*, *ApJ*, **651**, 142, 2006

[3] E.B. Fomalont, K.I. Kellermann, R.B. Partridge, R.A. Windhorst, E.A. Richards, *The Microjansky Sky at 8.4 GHz*, *AJ*, **123** 2402, 2002

[4] E.B. Fomalont, K.I. Kellermann, L.L. Cowie, P. Capak, A.J. Barger, R.B. Partridge, R.A. Windhorst, E.A. Richards, *The Radio/Optical Catalog of the SSA 13 Field*, *ApJS*, **167**, 103, 2006

[5] P. Ciliegi et al., *The VVDS-VLA deep field. II. Optical and near infrared identifications of VLA S1.4 GHz>80 µJy sources in the VIMOS VLT deep survey VVDS-02h field*, *A&A*, **441**, 879, 2005

[6] V. Smolcić, et al., *A New Method to Separate Star-forming from AGN Galaxies at Intermediate Redshift: The Submillijansky Radio Population in the VLA-COSMOS Survey*, *ApJS*, **177**, 14, 2008

[7] J.J. Condon, *Radio emission from normal galaxies*, *ARA&A*, **30**, 575, 1992

[8] R.J. Ivison, et al., *The far-infrared/radio correlation as probed by Herschel*, *A&A*, **518**, L31, 2010

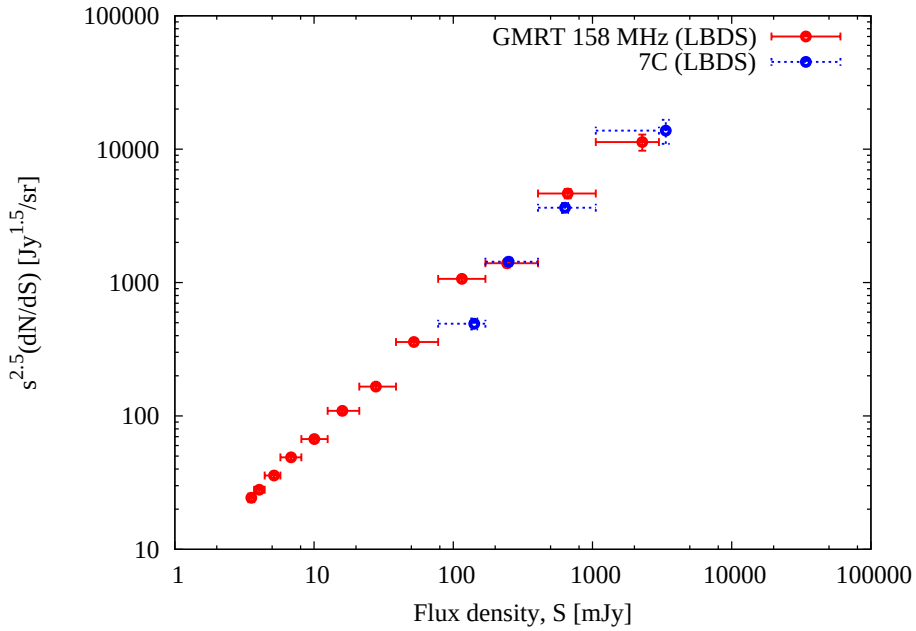

Figure 9: The normalized differential source counts at 150 MHz reproduced from Ishwara-Chandra et al. [17].

[9] P. Ranalli, A. Comastri, G. Setti, *The 2-10 keV luminosity as a Star Formation Rate indicator*, *A&A*, **399**, 39, 2003

[10] G. Miley, C. De Breuck, *Distant radio galaxies and their environments*, *A&ARv*, **15**, 67, 2008

[11] G. Giovannini, A. Bonafede, L. Feretti, F. Govoni, M. Murgia, F. Ferrari, G. Monti, *Radio halos in nearby (z<0.4) clusters of galaxies*, *A&A*, **507**, 1257, 2009

[12] D.J. Saikia, M. Jamrozy, *Recurrent activity in Active Galactic Nuclei*, *BASI*, **37**, 63, 2009

[13] S.K. Sirothia, M. Dennefeld, D.J. Saikia, H. Dole, F. Ricquebourg, J. Roland, *325-MHz observations of the ELAIS-N1 field using the Giant Metrewave Radio Telescope*, *MNRAS*, **395**, 269, 2009

[14] T. Garn, D.A. Green, J.M. Riley, P. Alexander, *A 610-MHz survey of the ELAIS-N1 field with the Giant Metrewave Radio Telescope - observations, data analysis and source catalogue*, *MNRAS*, **383**, 75, 2008

[15] N. A. Miller, E.B. Fomalont, K.I. Kellermann, V. Mainieri, C. Norman, P. Padovani, P. Rosati, P. Tozzi, *The VLA 1.4 GHz Survey of the Extended Chandra Deep Field-South: First Data Release*, *ApJS*, **179**, 114, 2008

[16] M.H. Wieringa, *PhD thesis*, Rijksuniversiteit Leiden, 1991

[17] C.H. Ishwara-Chandra, S.K. Sirothia, Y. Wadadekar, S. Pal, R. Windhorst, *Deep GMRT 150-MHz observations of the LBDS-Lynx region: ultrasteep spectrum radio sources*, *MNRAS*, **405**, 436, 2010

[18] S.K. Sirothia, D.J. Saikia, C.H. Ishwara-Chandra, N.G. Kantharia, *Deep low-frequency observations with the Giant Metrewave Radio Telescope: a search for relic radio emission*, *MNRAS*, **392**, 1403, 2009